JOURNAL OF PETROLEUM AND MINING
مجلة النفط والتعدين

Numerical Investigation of Hydrogen Flame Shape and Structure

Anmar A. Dhaaeif [1*], Muyassar E. Ismaeel [2] and Amir S. Dawood [3]

[1] *Department of Petroleum Reservoir Engineering, Collage of Petroleum and Mining engineering, University of Mosul, Iraq*

[2] *Department of Sustainable Energy Engineering, Collage of engineering, University of Mosul, Iraq*

[3] *Department of Mechanical Engineering, Collage of engineering, University of Mosul, Iraq*

Article information

Article history:
Received: Mar 26, 2025

Revised: Apr 06, 2025

Accepted: Jun 24, 2025

Available Online: Jul 01, 2025

Keywords:
Hydrogen combustion
LES
Swirl stabilization
turbulent flame
Jet flame

Correspondence:
Name: **Anmar A. Dhaaeif**
anmar.22enp63@student.uomosul.edu.iq

ABSTRACT

Hydrogen combustion is a promising alternative to fossil fuels, aiding decarbonization and pollution reduction. However, its unique properties pose challenges in flame stability, flashback, and NOx emissions. This study examines swirl-stabilized non-premixed hydrogen flames using Large Eddy Simulation (LES) to understand flame dynamics, stabilization, and emissions. Using the Hydrogen Low NOx (HYLON) burner from IMFT, the study analyzes attached and lifted flames under turbulent conditions at an equivalence ratio of 0.45. Fuel flow rates are 0.032 g/s and 0.08 g/s, and air flow rates are 2.41 g/s and 6.03 g/s for the attached (case A) and lifted (case L) flames, respectively. Simulations validated against Particle Image Velocimetry (PIV) data show strong agreement in velocity distribution and flow structures. The central and outer recirculation zones play key roles in flame stability and NOx formation. Results reveal that lifted flames emit less NOx due to better mixing, while attached flames produce more NOx due to prolonged high-temperature exposure. This research advances hydrogen combustion knowledge, supporting the transition to clean energy solutions by addressing key challenges in combustion modeling, emission control, and flame stability.

DOI: **********, ©Authors, 2025, College of Petroleum and Mining Engineering, University of Mosul.

التحليل العددي لشكل وبنية لهب الهيدروجين

انمار علي الجبوري[1,*], ميسر ادريس اسماعيل[2], امير سلطان داوود[3]

[1] *قسم هندسة المكامن النفطية، كلية هندسة النفط والتعدين، جامعة الموصل، الموصل، العراق*

[2] *قسم هندسة الطاقة المستدامة، كلية الهندسة، جامعة الموصل، العراق*

[3] *قسم الهندسة الميكانيكية، كلية الهندسة، جامعة الموصل، الموصل، العراق*

معلومات الارشفة

تاريخ الارشفة:

تاريخ الاستلام :مارس 26، 2025

تاريخ المراجعة :أبريل 6، 2025

تاريخ القبول :يونيو 24، 2025

تاريخ النشر الإلكتروني :يوليو 1، 2025

الكلمات المفتاحية:

تحاليل السرعة

احتراق الهيدروجين

المحاكاة العددية للدوامات الكبيرة (LES)

تثبيت دوامي

لهب اضطرابي

لهب نفثي

المراسلة:

الاسم: **انمار علي الجبوري**

anmar.22enp63@student.uomosul.edu.iq

الملخص

يُعَدّ احتراق الهيدروجين خيارًا استراتيجيًا واعدًا ضمن منظومة التحوّل نحو مصادر طاقة نظيفة، لما يتميز به من قدرة عالية على تقليل الانبعاثات الكربونية والملوثات البيئية المصاحبة لاحتراق الوقود الأحفوري. ومع ذلك، فإن الخصائص الفيزيائية والكيميائية الفريدة للهيدروجين تطرح تحديات جوهرية في ما يتعلق بثباتية اللهب، واحتمالية الارتداد، ومستويات انبعاثات أكاسيد النيتروجين (NOx). تهدف هذه الدراسة إلى إجراء تحليل عددي دقيق لسلوك لهب الهيدروجين غير المُسبق الخلط والمُثبت بواسطة دوامة هوائية، وذلك باستخدام تقنية المحاكاة العددية للدوامات الكبيرة (LES)، بهدف استقصاء ديناميكية اللهب وآليات تثبيته وأنماط الانبعاثات الناتجة. تم اعتماد موقد الهيدروجين منخفض الانبعاثات (HYLON)، المطوَّر في معهد ميكانيكا الموائع بمدينة تولوز (IMFT)، كنموذج تطبيقي للدراسة. تم تحليل نوعين من اللهب: اللهب الملتصق باللهب الرئيسي (الحالة A) واللهب المرتفع (الحالة L)، تحت ظروف جريان اضطرابية، بنسبة مكافئة بلغت 0.45. بلغت معدلات تدفق الوقود 0.032 غ/ثانية و0.08 غ/ثانية، بينما كانت معدلات تدفق الهواء 2.41 غ/ثانية و6.03 غ/ثانية للحالتين A و L على التوالي. أظهرت نتائج المحاكاة تطابقاً ملحوظاً مع البيانات التجريبية المستخلصة باستخدام تقنية تصوير الجسيمات عبر السرعة (PIV)، سواء من حيث توزيع السرعة أو بنية الجريان. أوضحت الدراسة أن منطقتي إعادة الدوران المركزية والمحيطية تؤديان دوراً محورياً في تثبيت اللهب والتحكم في معدلات توليد أكاسيد النيتروجين. كما كشفت النتائج أن اللهب المرتفع يمتاز بانخفاض ملحوظ في انبعاثات NOx، نتيجة تعزيز الخلط بين الوقود والمؤكسد، مقارنة باللهب الملتصق الذي يرتبط بانبعاثات أعلى نتيجة التعرض المستمر لدرجات حرارة مرتفعة. تُسهم هذه النتائج في تعزيز الفهم العلمي لآليات احتراق الهيدروجين، وتُشكّل قاعدة معرفية داعمة لجهود تطوير تقنيات احتراق نظيفة وفعالة، من خلال تحسين نماذج الاحتراق، وتقنيات السيطرة على الانبعاثات، وضمان ثباتية الأداء الحراري للأنظمة.

DOI: **********,

Introduction

Fuel combustion has served as a primary energy source essential for human advancement since the discovery of fire. To this day, combustion technologies continue to dominate global energy production, accounting for nearly 90% of the world's primary energy, playing a vital role across various sectors including industry, transportation, and space exploration (Otway, 2020). Historically, economic growth and societal development have been directly linked to increased energy consumption, particularly evident during the Industrial Revolution, marked by the extensive utilization of fossil fuels (coal, oil, and natural gas) to satisfy rising industrial, transportation, and electricity demands. Currently, fossil fuels still provide approximately 81% of global energy needs ((IEA), 2025; Martinez & Jiang, 2013). However, this heavy reliance has led to significant environmental challenges, notably climate change and air pollution, largely due to greenhouse gas emissions such as carbon dioxide (CO2) and nitrogen oxides (NOx), which have increased dramatically by about 46% since 1990 ((IEA), 2025). This warming phenomenon, commonly known as the greenhouse effect, was initially proposed by Joseph Fourier in 1827 and later experimentally confirmed by John Tyndall in 1859 (Marragou, 2023). To combat these environmental issues, global initiatives like the Paris Climate Agreement have emerged, aiming to restrict the increase in Earth's average temperature to below two degrees Celsius compared to pre-industrial levels (European Commission, 2022) Hydrogen, produced through renewable methods such as solar, wind, or nuclear energy, presents itself as a sustainable alternative fuel. Its combustion uniquely yields no carbon dioxide emissions, producing only water vapor (Chiesa et al., 2005; Dincer, 2012). Nevertheless, the utilization of hydrogen as a fuel introduces significant technical challenges due to its inherent properties, including rapid combustion speed and wide flammability limits, leading to flame instabilities, flashback phenomena, and elevated NOx emissions under certain combustion conditions (Bouvet et al., 2013; Milton & Keck, 1984). Various engineering approaches have been adopted to address these challenges, with swirl flow combustion systems being particularly notable. By generating a Central Recirculation Zone (CRZ), swirl flow promotes better fuel-air mixing, thereby enhancing flame stability (Galley et al., 2011; Lu et al., 2023). However, swirl-based systems are not without their own set of complications, such as vortex breakdown and Precessing Vortex Core (PVC) oscillations, phenomena that necessitate further investigation for effective control and optimal utilization (A. K. Gupta et al., 1984). Numerical modeling, particularly Large Eddy Simulation (LES), has increasingly gained prominence as a critical tool to deepen our understanding of hydrogen combustion dynamics. LES allows detailed analysis of complex interactions among turbulent flow, chemical reactions, and flame structures, significantly reducing the need for costly and time-consuming experimental tests. Consequently, LES has facilitated the development of safer, more efficient, and environmentally friendly combustion technologies. Despite considerable progress, existing literature reveals persistent knowledge gaps, especially in fully understanding and mitigating combustion instabilities, flashback phenomena, and NOx formation mechanisms in hydrogen combustion systems. Therefore, the current study aims to fill these gaps through comprehensive LES-based numerical simulations, specifically analyzing hydrogen jet flame behavior to enhance flame stability and reduce emissions. Such research is crucial for advancing hydrogen combustion technologies and supporting the global transition towards sustainable, low-carbon energy systems. Hydrogen combustion exhibits unique characteristics compared to conventional hydrocarbon fuels, characterized by high combustion speed and a wide flammability range, enhancing combustion efficiency but increasing the likelihood of

instabilities and flame flashback (Lipatnikov & Sabelnikov, 2020). Studies such as (Fairweather et al., 2009) have demonstrated that the addition of hydrogen to methane increases flame temperature and combustion speed. Swirl flows are extensively employed to enhance flame stability and improve fuel-air mixing. The swirl flow creates a Central Recirculation Zone (CRZ), aiding flame stabilization away from the injector lip (Beér & Chigier, 1972; Chigier & Bee´r, 1964; Chigier & Chervinsky, 1967a, 1967b). Studies by (Patel & Shah, 2019) and (Zhen et al., 2010) indicate that increasing the swirl number shortens flame length and reduces emissions. Conversely, (Ilbaş et al., 2016) reported that excessive swirl intensification leads to increased nitrogen oxide (NOx) emissions. Although hydrogen is considered a clean fuel, it leads to NOx emissions due to high combustion temperatures (Marragou, 2023). Various studies, including those (Lan et al., 2024), have indicated that higher hydrogen proportions in fuel mixtures significantly increase flame temperatures, creating hotspots that elevate NOx emission rates. To reduce these emissions, technologies such as partial air and steam injection have been developed to lower combustion temperatures (Reichel et al., 2015; Truffin et al., 2024). Flashback phenomena represent one of the main challenges in hydrogen combustion systems, closely linked to hydrogen's highly reactive flame properties (Sommerer et al., 2004). Researchers such as (Eichler & Sattelmayer, 2012; Ebi et al., 2021; Reichel & Paschereit, 2017; Duan et al., 2014) have investigated various methods to mitigate this phenomenon by controlling injection velocity, cooling, and selecting materials with suitable thermal conductivity.

Stabilizing turbulent flames in combustion systems requires an in-depth understanding of stability mechanisms (A. Gupta, 2000; A. K. Gupta et al., 1999). Several models explaining turbulent flame stabilization mechanisms have been developed. Recent studies by (Marragou et al., 2023) and (Aniello et al., 2023a) have proven the effectiveness of the dual-swirl HYLON injector in achieving excellent flame stability and reducing thermal emissions.

Nomenclature		**Greek symbols**		
S_a	**Air swirl number**	**ρ**	**Filtered density**	**(kg/m³)**
S_h	**Hydrogen swirl number**	**$\bar{P}$**	**Filtered pressure**	**(Pa)**
		τ_{ij}	**Sub-grid stress tensor**	**(N/m²)**
T	**Temperature (K)**	**κ**	**Sub-grid kinetic energy**	**(m²/s²)**
NO_x	**Nitrogen oxides (ppm or kg/m³)**	**ε**	**Sub-grid dissipation rate**	**(m²/s³)**
		ϕ	**Equivalence ratio**	
CRZ	**Central Recirculation Zone**	**ϕ_{st}**	**Stoichiometric equivalence ratio**	
ORZ	**Outer Recirculation Zone**	**Δ**	**Filter size or grid size**	**(m)**
IRZ	**Inner Recirculation Zone**	**μ_{sgs}**	**Subgrid viscosity**	**(Pa·s)**
LES	**Large Eddy Simulation**	**$\sigma_k, \sigma_\varepsilon$**	**Model constants for turbulence equations**	
SGS	**Subgrid-Scale**	**Ω_{steam}**	**Steam dilution ratio relative to air**	**(%)**
AMR	**Adaptive Mesh Refinement**	**τ**	**Time scale**	**(s)**
CFD	**Computational Fluid Dynamics**	**C_k, C_ε**	**Model constants for subgrid viscosity**	
DRGEP	**Directed Relation Graph with Error Propagation**	**L_{ij}**	**Leonard stress tensor**	**(N/m²)**
PIV	**Particle Image Velocimetry**	**c_{ij}**	**Dynamic structure coefficient tensor**	

Physical configuration

The HYLON burner geometry shown in Figure 1a, as described by (Aniello et al., 2023a), is designed to optimize hydrogen-air combustion through a dual-swirl injector system and a well-defined combustion chamber. The air is supplied through an annular channel with an external diameter of 18 mm, featuring a radial swirler composed of eight cylindrical vanes, each 4 mm in diameter and tilted at a 42° angle to the radial direction, achieving an air swirl number of Sa=0.65, as illustrated in Figure 1b. This configuration creates strong rotational flow and a central recirculation zone (CRZ), enhancing flame stability and reducing flashback risks. Hydrogen is injected through a central tube with a 6mm diameter and 2mm wall thickness, equipped with an axial helicoidal swirler producing a hydrogen swirl number of Sh=0.60. The injector lip is recessed by 4 mm from the burner backplane to allow efficient pre-mixing of reactants before ignition. The combustion chamber has a square cross-section measuring 78 mm×78 mm, a length of 190 mm, and transitions to a circular nozzle of 73 mm diameter over a 39 mm length.

These design specifications were based on prior work by (Marragou, 2023), who investigated dual-swirl systems for hydrogen flames, and (Aniello et al., 2023a), who explored the stabilization mechanisms in swirling hydrogen flames. Key contributions include the aerodynamic stabilization of flames via inner recirculation zones (IRZ), reducing thermal stresses and improving pollutant control.

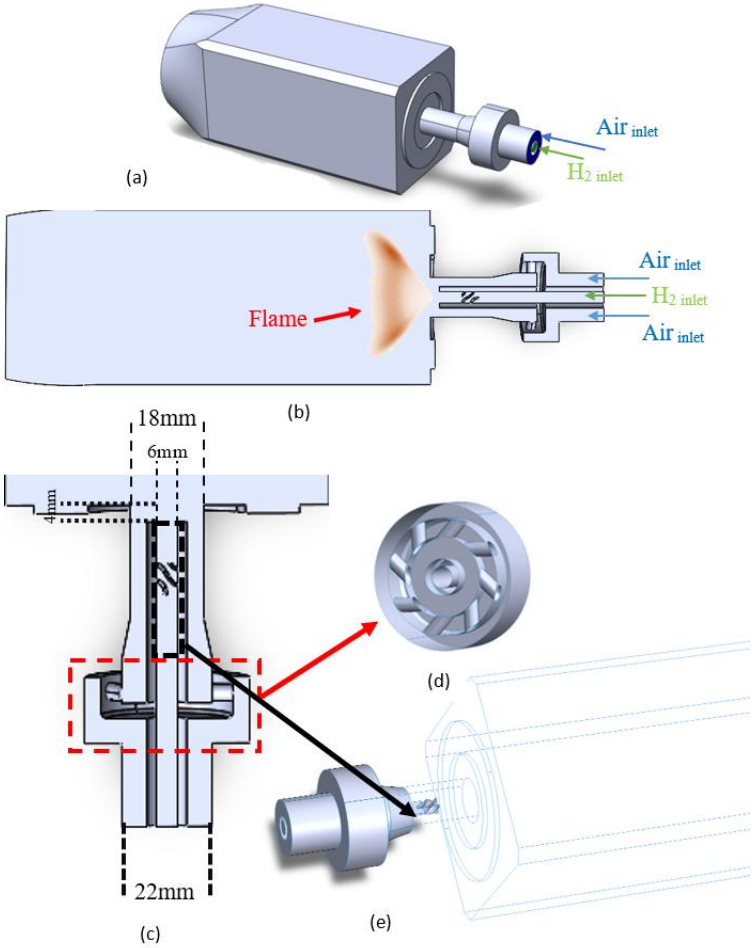

Fig. 1. The geometry of the burner under study: (a) 3D view of the burner, (b) cross-section of the burner depicts the inlets of air and hydrogen, (c) the inlets' dimensions, (d) Air swirler, and (e) hydrogen swirler.

Mathematical model

In this study, the simulation of turbulent hydrogen jet flames was performed using the Large Eddy Simulation (LES) approach within the CONVERGE CFD platform, incorporating detailed chemical kinetics, adaptive mesh refinement (AMR), and a two-equation subgrid-scale (SGS) turbulence model. LES was chosen for its ability to resolve the large energy-containing eddies in turbulent flows while modeling the smaller scales using SGS models, which is crucial for accurately capturing the fast, reactive nature of hydrogen flames. The filtered Navier–Stokes equations are the foundation of LES, where the momentum transport equation is written as

$$\frac{\partial(\bar{\rho}\tilde{u}_i)}{\partial t} + \frac{\partial(\bar{\rho}\tilde{u}_i\,\tilde{u}_j)}{\partial x_j} = -\frac{\partial \bar{P}}{\partial x_i} + \frac{\partial \bar{\sigma}_{ij}}{\partial x_j} - \frac{\partial \tau_{ij}}{\partial x_j} \qquad (1)$$

where:
$\bar{\rho}$ is the filtered density,
$\tilde{u}_i$ is the filtered velocity,
$\bar{P}$ is the filtered pressure,

$\bar{\sigma}_{ij}$ is the filtered viscous stress tensor,
τ_{ij} is the sub-grid stress tensor, representing the unresolved scales.
The sub-grid stress tensor is modeled as:

$$\tau_{ij} = 2\rho\kappa c_{ij} \qquad (2)$$

Where:
κ is the sub-grid kinetic energy,
c_{ij} is the dynamic structure coefficient tensor, defined as:

$$c_{ij} = \frac{L_{ij}}{L_{kk}} \qquad (3)$$

$L_{ij}$is the Leonard stress tensor, given by:

$$L_{ij} = \widehat{\tilde{u}_i \tilde{u}_j} - \widehat{\tilde{u}_i}\widehat{\tilde{u}_j} \qquad (4)$$

Here, $\widehat{\ }$ denotes a test filter operation, typically twice the size of the grid filter. In this case, the test filter is twice the size of the grid. It is worth noting that the subgrid-scale tensor model does not employ a subgrid-scale viscosity formulation for closure. Instead, the two-equation dynamic structure model extends the one-equation dynamic structure model by introducing an additional transport equation for subgrid-scale dissipation. This model relies on two transport equations: one for the subgrid-kinetic energy (k) as formulated by (Yoshizawa & Horiuti, 1985) and (Menon et al., 1996) and another for the sub-grid dissipation (ϵ) as expressed in (Richards et al., 2023)

The two-equation dynamic structure model solves two transport equations:
Sub-grid Kinetic Energy ($\bar{k}$):

$$\frac{\partial(\rho\bar{k})}{\partial t} + \frac{\partial(\rho\tilde{u}_i k)}{\partial x_i} = -\tau_{ij}\frac{\partial\tilde{u}_i}{\partial x_j} - \varepsilon + \frac{\partial}{\partial x_i}\left(\mu_{sgs}\frac{\partial k}{\sigma_k}\right) \qquad (5)$$

Where:
μ_{sgs} is the subgrid viscosity,
σ_k is a model constant.
Subgrid Dissipation (ε):

$$\frac{\partial(\bar{\rho}\varepsilon)}{\partial t} + \frac{\partial(\bar{\rho}\tilde{u}_i\varepsilon)}{\partial x_i} = \left(\frac{3C_\varepsilon\bar{\rho}\varepsilon}{2k}\right)P - \frac{3\bar{\rho}\varepsilon^2}{2k} + \frac{\partial}{\partial x_i}\left(\frac{\mu_{sgs}}{\sigma_\varepsilon}\frac{\partial\varepsilon}{\partial x_i}\right) + \frac{\bar{\rho}\varepsilon}{l_f}\left(\frac{\Delta_f - \Delta_g}{\tau}\right) \qquad (6)$$

where:
$\bar{\rho}$ is the subgrid production,
Δ_f is the local filter size,
$\Delta_g$is the local grid filter size,
The local filter size is expressed as:

$$\Delta_f = C_\varepsilon\frac{\bar{k}^{\frac{3}{2}}}{\varepsilon} \qquad (7)$$

The time scale τ is defined by:

$$\boldsymbol{\tau = \frac{C_\tau k}{\varepsilon}} \qquad (8)$$

In CONVERGE, the constant Cτ is set to 0.5.

In the two-equation formulation, the local filter size does not instantly align with the local grid size but instead evolves dynamically over time. The subgrid-scale viscosity is formulated as:

$$\boldsymbol{\mu_{sgs} = C_k \bar{\rho} k^{\frac{1}{2}} \Delta_f = C_k C_\varepsilon \frac{\bar{\rho} k^2}{\varepsilon}} \qquad (9)$$

Here, $\boldsymbol{C_\varepsilon}$ and $\boldsymbol{C_k}$ are constants specific to the model. Simulations were conducted at standard atmospheric pressure (1 atm) and inlet temperatures of 300 K for both hydrogen and air. A global equivalence ratio of φ = 0.45 was selected to promote lean combustion, which enhances thermal efficiency and reduces NOx formation. The flow field was modeled under two configurations: an attached flame with hydrogen and air mass flow rates of 3.2×10^{-5} kg/s and 2.41×10^{-3} kg/s, respectively, this flame defined as a flame stabilization regime in which the flame remains anchored very close to the central injector nozzle, such that the chemical reaction initiates immediately upon the fuel's exit, with virtually no gap between the injector and the ignition zone and a lifted flame with flow rates of 8.0×10^{-5} kg/s and 6.03×10^{-3} kg/s. This designation arises from the fact that the flame stabilizes at a location removed from the injector nozzle. The full operation conditions are presented in Table 1. Swirl injection was used in both fuel and air channels to promote enhanced mixing and flame stabilization through central and outer recirculation zones. For combustion modeling, the SAGE solver within CONVERGE was used to solve detailed chemical kinetics through CHEMKIN-formatted mechanisms, employing the CVODE solver from the SUNDIALS suite to handle stiff ODEs arising in hydrogen combustion. The chemical mechanism adopted was the reduced mechanism by Capurso et al. (Capurso et al.,2023), consisting of 15 species and 47 reactions, specifically optimized for accurate NOx prediction. This mechanism includes thermal and prompt NOx pathways involving intermediate species like N_2O and NNH, and has been validated against the comprehensive CRECK mechanism with 159 species and 1459 reactions. It has also been benchmarked across a wide range of conditions, showing excellent agreement, especially as further validated by (Shahin, 2024). For computational efficiency, chemical reactions were only activated above a minimum cell temperature of 600 K, and a hydrogen species concentration threshold of 10^8 was imposed in low-temperature cells to maintain active chemistry. To accurately resolve flame structure and high-gradient regions, Adaptive Mesh Refinement (AMR) was employed, with the refinement criterion based on local temperature gradients, achieving minimum cell sizes of approximately 0.225 mm near the flame front. Furthermore, CONVERGE's Fixed Embedding technique allowed accurate representation of rotating components like swirlers, maintaining mesh quality without full regeneration at each time step. This overall modeling strategy, combining the LES framework with detailed kinetics, dynamic meshing, and well-defined operating conditions, enabled the accurate capture of turbulent structures, flame anchoring behavior, and pollutant formation in hydrogen combustion systems.

Table 1: Operation Conditions

Case	Type of flame	Mass flow rate of hydrogen (kg/s)	Mass flow rate of Air (kg/s)	Pressure (Atm)	Inlet of hydrogen (K)	Inlet of Air (K)	Ω_{steam}
I	Attached flame (flame A)	$3.2\text{x}10^{-5}$	$2.41\text{x}10^{-3}$	1 atm	300	300	0%
II	Lifted flame (flame L)	$8\text{x}10^{-5}$	$6.03\text{x}10^{-3}$	1 atm	300	300	0%

Numerical procedure

The numerical simulation was performed using CONVERGE CFD, a solver specifically designed for reactive flow applications with automated meshing and built-in support for turbulence and combustion modeling. The simulation process followed a structured sequence, beginning with geometry import and case setup through CONVERGE Studio. The burner geometry, including the swirl injector and surrounding domain, was defined using CAD tools and imported into the simulation environment. Boundary conditions were applied to each region of the domain, specifying mass flow rates, temperature, turbulence levels, and swirl characteristics at the inlets, as well as pressure boundaries at the outlet. Following domain setup, CONVERGE's fully automated mesh generation system was used. The base grid size was selected to ensure efficient coverage of the entire domain, while key zones—such as the injector and flame region—were targeted with finer local refinement using embedded regions. Dynamic Adaptive Mesh Refinement (AMR) was then enabled to respond to evolving flow structures during the simulation, ensuring localized resolution of steep gradients without manual remeshing. The solver settings were configured to activate detailed combustion chemistry and LES-based turbulence modeling. The chemical mechanism and transport models were linked via CHEMKIN input, and the solver automatically handled integration and species coupling. Simulation time advancement was controlled using a variable time step algorithm, with the minimum time step set to 1×10^{-6} s and the maximum allowed step set to 1×10^{-4} s, maintaining accuracy and stability near reactive fronts. As utilized within the CONVERGE software, the modified density-based Pressure Implicit with Splitting of Operator (PISO) algorithm begins with a predictor phase, in which the momentum equations are solved explicitly using the available pressure field to compute a provisional velocity field. This initial step does not yet satisfy mass conservation, but serves as a first approximation to the flow field. Following this, the algorithm enters a corrector phase, where a pressure correction equation is derived from the continuity equation and solved iteratively. This step updates both the pressure and velocity fields to enforce global mass conservation. Multiple corrector steps may be executed per time step to improve pressure–velocity coupling, particularly under compressible and transient conditions. In CONVERGE's implementation, the method is enhanced for density-based formulations, allowing robust handling of strong density gradients due to combustion. Stability is further reinforced using relaxation factors and residual-based convergence criteria. This tight integration between the pressure solver and the reacting flow field supports accurate simulation of hydrogen combustion. Initial conditions were applied uniformly, and the simulation was allowed to evolve toward a statistically steady state. For the reactive cases, the simulations were run for a physical time of 8 milliseconds, while non-reactive simulations were extended to 12

milliseconds to ensure sufficient flow development and capture of key transient behaviors. During the run, data were sampled at selected planes and volumes to extract velocity, temperature, species concentration, and flame location.

Results and discussion

Validation

The available experimental Particle Image Velocimetry (PIV) dataset was utilized to compare numerical simulation results with experimental data in the axial plane of the combustion chamber. A two-dimensional (2D) contour was created to display the data, alongside the corresponding Large Eddy Simulation (LES) simulation results, as illustrated in (Fig. 2). The results showed a relatively good agreement between the axial and radial velocity values extracted from the numerical and experimental files in the primary vortex region. However, some minor discrepancies were observed, which could be attributed to factors such as the mesh size used in the simulation, which may affect the accuracy of the results. Velocity plays a fundamental role in defining recirculation zones, which are crucial for shaping and stabilizing the flame in reactive environments. These zones facilitate the redistribution of fuel and air within the chamber, enhancing the combustion process and ensuring its sustainability. They also serve a dual function by acting as a fuel source through recirculating unburned reactants into the combustion zone while simultaneously providing thermal energy to support flame stability and prevent extinction. This dynamic makes recirculation a key factor in designing high-efficiency combustion systems, particularly in industrial applications, gas turbines, and hydrogen-fueled propulsion systems (Tummers, 2009; Aniello, 2023)

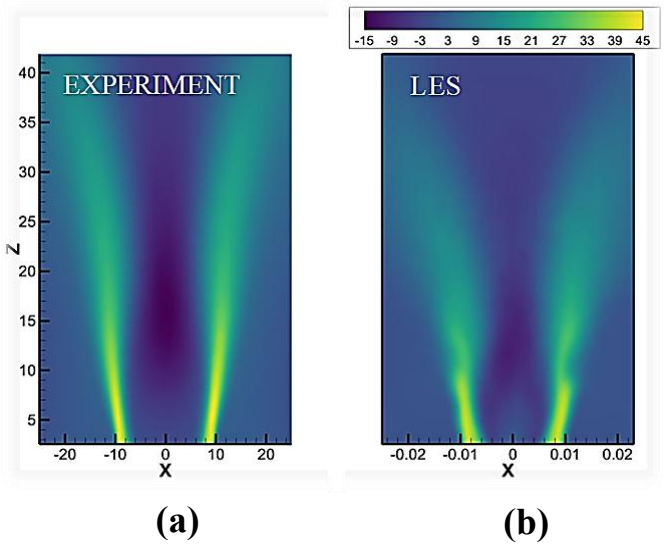

Fig. 2. Comparison of mean velocity fields between (a) Experiment and (b) LES results in non-reactive flow

The central recirculation zone (CRZ) can be identified by the dark green region where axial velocity values are negative, indicating a reverse flow that redirects the mixture toward the flame core. Meanwhile, the outer recirculation zone (ORZ) appears as a light green region in the left and right corners of the experimental domain. This zone helps maintain flow stability

by reducing disturbances in the outgoing jet and optimizing the fuel-air mixing process before ignition. A validation between experimental results and numerical simulations reveals a good agreement in the distribution of CRZ and ORZ, confirming the reliability of the numerical model in representing real combustion dynamics. Figures 3 and 4 present a validation between experimental data and LES simulation results for reactive flows at heights z = 5 mm and z = 15 mm, which approximately represent the middle and upper flame regions. This comparison focuses on analyzing flow structure and assessing the accuracy of numerical models in predicting velocity distribution and turbulence fields. The LES simulation shows good agreement with experimental data in both scenarios, accurately capturing the size and intensity of the inner recirculation zone (IRZ) through the predicted axial velocity distribution Uz. Additionally, The agreement between experimental and numerical results for radial velocity Ur at both heights demonstrates that the LES model effectively captures the vortex flow opening angle, indicating an improved representation of injection dynamics.

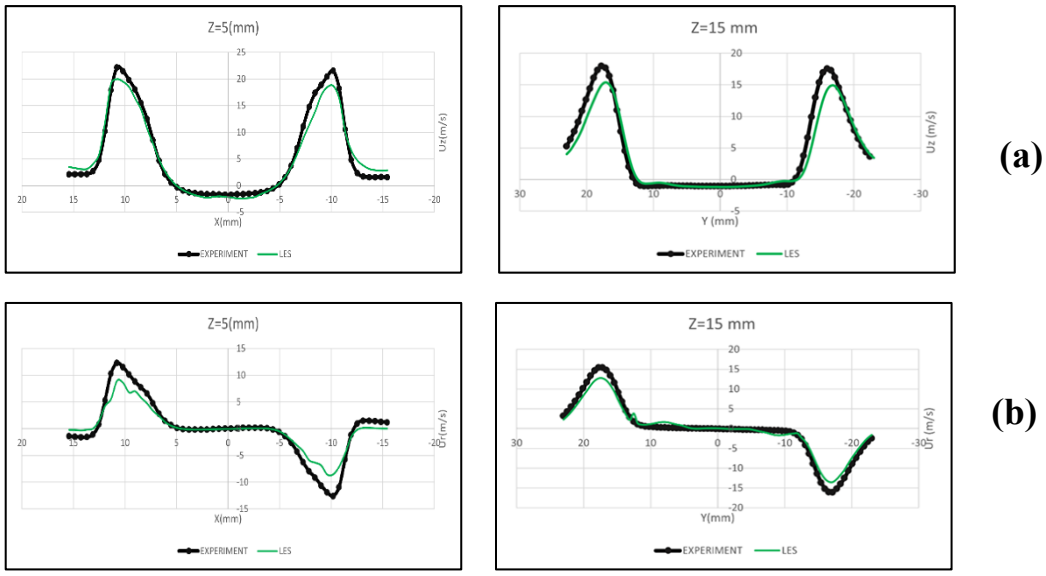

Fig. 3. validation between velocity PIV data (depicted by symbols) of flame A at Z=5 mm and Z=15mm on the axial plane versus LES results for a) the mean axial UZ and b) radial velocity Ur.

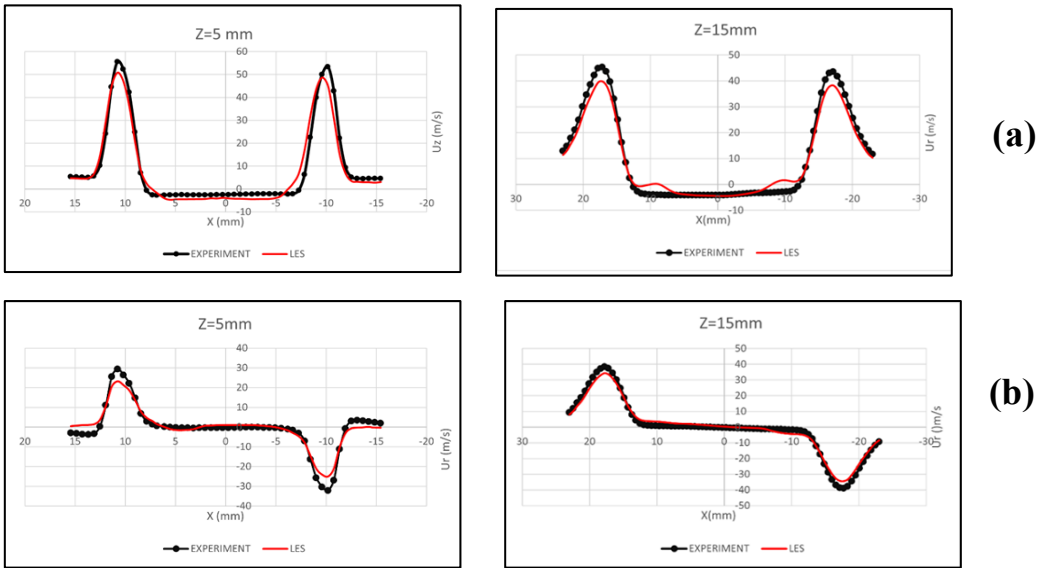

Fig. 4. validation between velocity PIV data (depicted by symbols) of flame A at Z= 5 mm and Z= 15mm on the axial plane versus LES results for (a) the mean axial UZ and (b) radial velocity Ur.

Velocity field

The velocity magnitude contours in Figure 5 highlight the effectiveness of LES in accurately capturing complex flow characteristics in regions with high swirl intensity, which are challenging to replicate due to the small-scale turbulent fluctuations. The results reveal the presence of large eddies generated by the swirling flow, particularly near the entrance of the combustion chamber. These eddies are critical in promoting fuel-air mixing and enhancing combustion efficiency. The maximum velocity is observed near the mixing blades inside the hydrogen fuel transport pipe, just before the combustion chamber inlet. These blades induce a rotational motion (swirl) in the fuel flow, intensifying the interaction between the fuel and air streams, thereby improving mixing, momentum transfer, and jet stability. The contours also show the development of a distinct shear layer at the nozzle orifice, where the fuel and air jets transition into a region of momentum exchange with the surrounding fluid. This shear layer is characterized by turbulence and viscous interactions, leading to the formation of vortices and flow instabilities. These features enhance mixing and entrainment of ambient fluid into the jet. As the flow progresses downstream, the shear layer broadens, and the velocity profile becomes more uniform, indicating the dissipation of the jet's kinetic energy. This dissipation occurs through turbulent diffusion and viscous dissipation mechanisms, converting the jet's energy into smaller-scale turbulent motions and heat. Over time, the jet loses coherence and integrates with the surrounding flow, demonstrating the intricate dynamics of jet development, mixing, and eventual dissipation in a high-swirl environment.

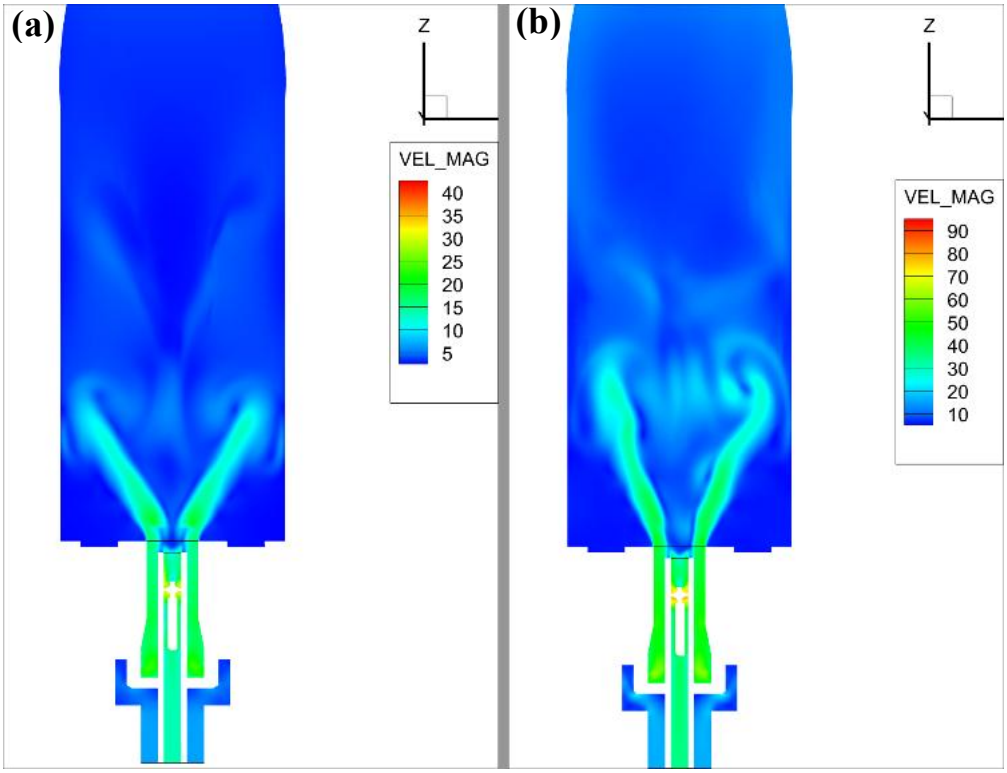

Fig. 5. Velocity magnitude of (A) Flame A, and (B) Flame L.

Temperature

Figure 6 illustrates the temperature distribution in the combustion chamber for both cases, highlighting some advanced aspects of the combustion process. At the core of the flame, a very hot nucleus appears, where temperatures reach approximately 2300 K.

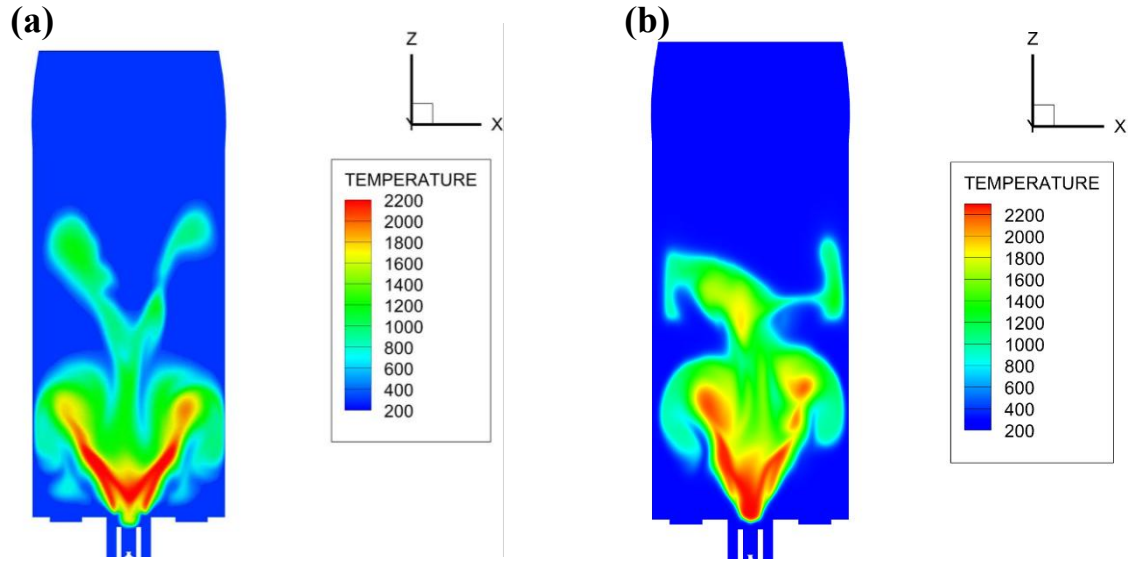

Fig. 6. 2D contour plot of the temperature for both flames, a) Flame A and b) Flame L

This central region represents the site where most chemical reactions occur, releasing a significant amount of thermal energy. Surrounding this nucleus are lower-temperature regions

where heat is gradually. Figure 7 presents the temperature distribution and equivalence ratio contours in the flame, emphasizing the dynamic relationship between the fuel-air mixture and combustion efficiency. The high-temperature regions near the base of the flame (up to 2300 K) align with the stoichiometric equivalence ratio line (ϕst), which is positioned at the center of the flame, representing the primary combustion zone characterized by high stability and efficiency. The equivalence ratio gradient in Figure 8 shows a transition from a rich mixture (ϕ > 1) near the base of the flame to a lean mixture (ϕ < 1) at the flame's edges, with the stoichiometric equivalence ratio (ϕst = 1) occurring at the flame's core. This gradient highlights the interaction between fuel and air across different regions, ensuring balanced combustion dynamics. The temperature and equivalence ratio distributions provide clear insight into the flame's internal structure and the critical role of mixture composition in achieving efficient combustion.

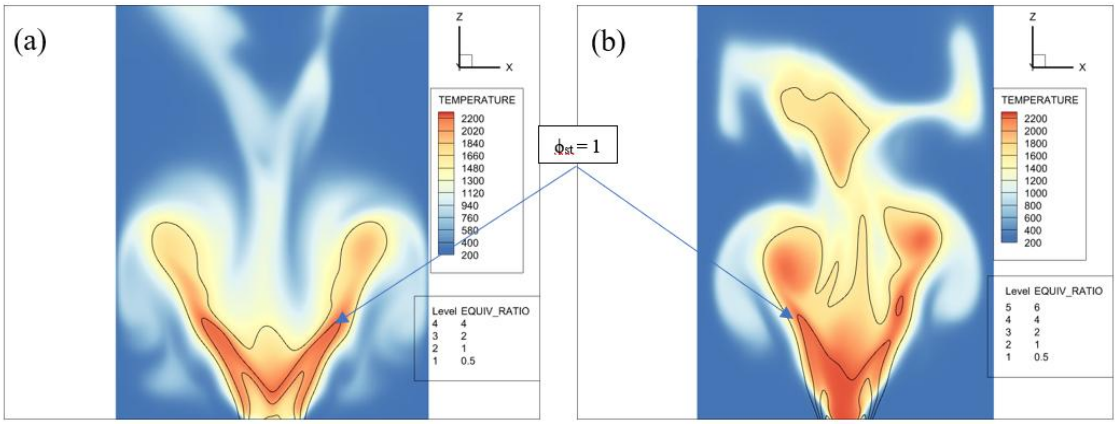

Fig. 7. 2D contour plot of the temperature for both flames: (a) Flame A and (b) Flame L, with isolines of local equivalence ratio serving to emphasize the mixture distribution concerning the flame position.

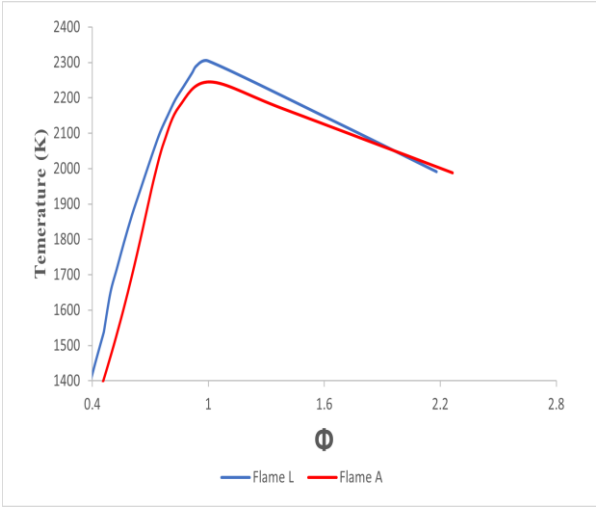

Fig. 8. relation between local equivalence ratio and temperature

Flame shape

Figure 6 shows two different flame configurations, M and V. The attached flame, as shown in Figure 6 (a), exhibits a characteristic thermal distribution with a clear M shape. This

configuration reflects a local concentration of chemical reactions and high thermal density within the central core near the injector nozzle, which enhances the efficiency of chemical reactions in the central zone. However, this high thermal density can contribute to an increased risk of hotspot formation, which in turn increases the likelihood of nitrogen oxide (NOx) formation. Figure 10 shows the flame formation farther from the nozzle, then it begins to spread downward to the burner nozzle, forming the letter M. This shape difference is due to the difference in flow rate of the two flames, and therefore, the recycling regions occur at different positions relative to the nozzle. Flame A has a lower flow rate, so (CRZ) are farther from the nozzle, as shown in Figure 9. Since the speed is low, this allows for greater residence time, ensuring that combustion reactions occur at both ends of the flame center, as shown in Figure 16, where a ring appears around the flame center, and this ring begins to spread downward toward the nozzle. Thus, it is called the attached flame, while the lifted flame, which appears in Figures 12 and 6 (b), has the flame core at the lower part of the ignition zone, and the flame starts to rise from the edges, forming the letter V. This is, as mentioned, a result of the different positions of the recycling regions, which in the case of the lifted flame, are closer to the nozzle, as shown in Figure 9 (b). As a result, the flame spreads upward from the center, moving away from the nozzle, and is therefore called the lifted flame, taking a conical shape as shown in Figure 13.

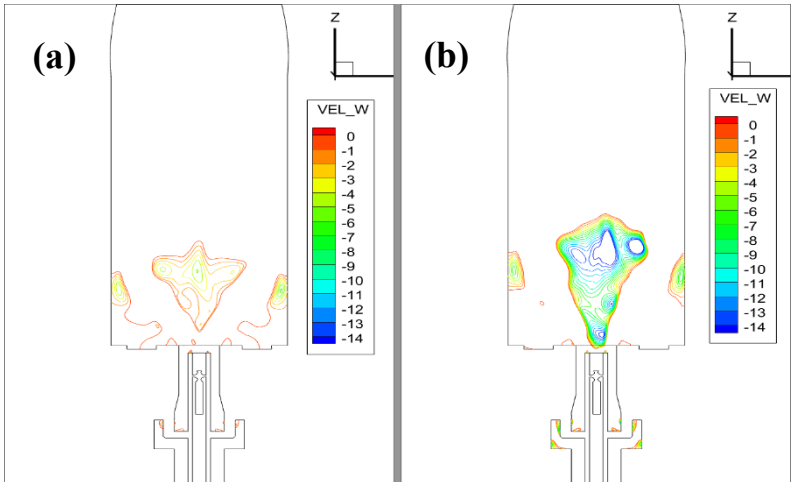

Fig. 9. Axial velocity isoline where CRZ appears in (a) Flame A and (b) Flame L

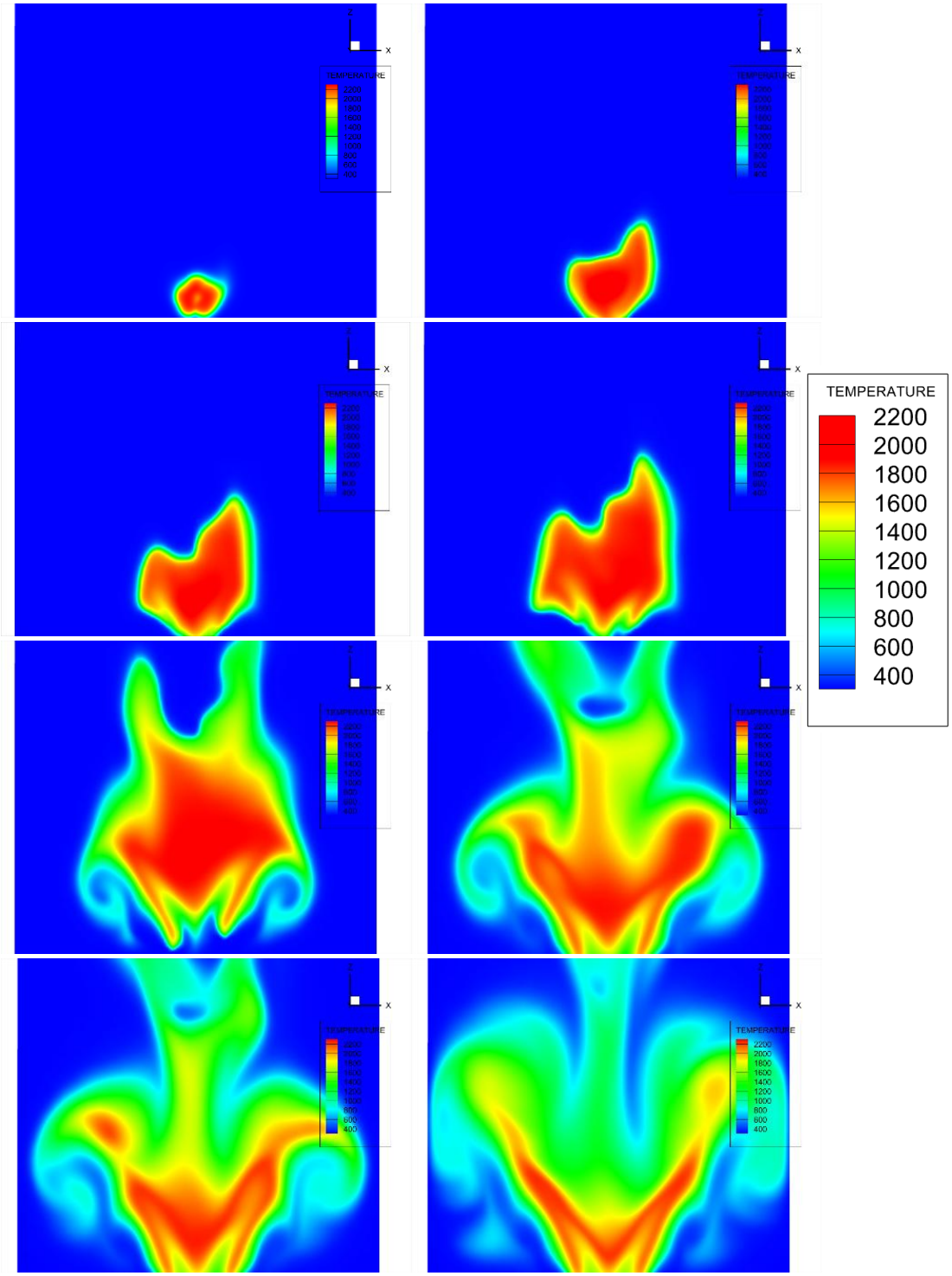

Fig. 10. Instantaneous temperature Contours for attached flame in X-Z plan at y=0 from 1-8 ms time step

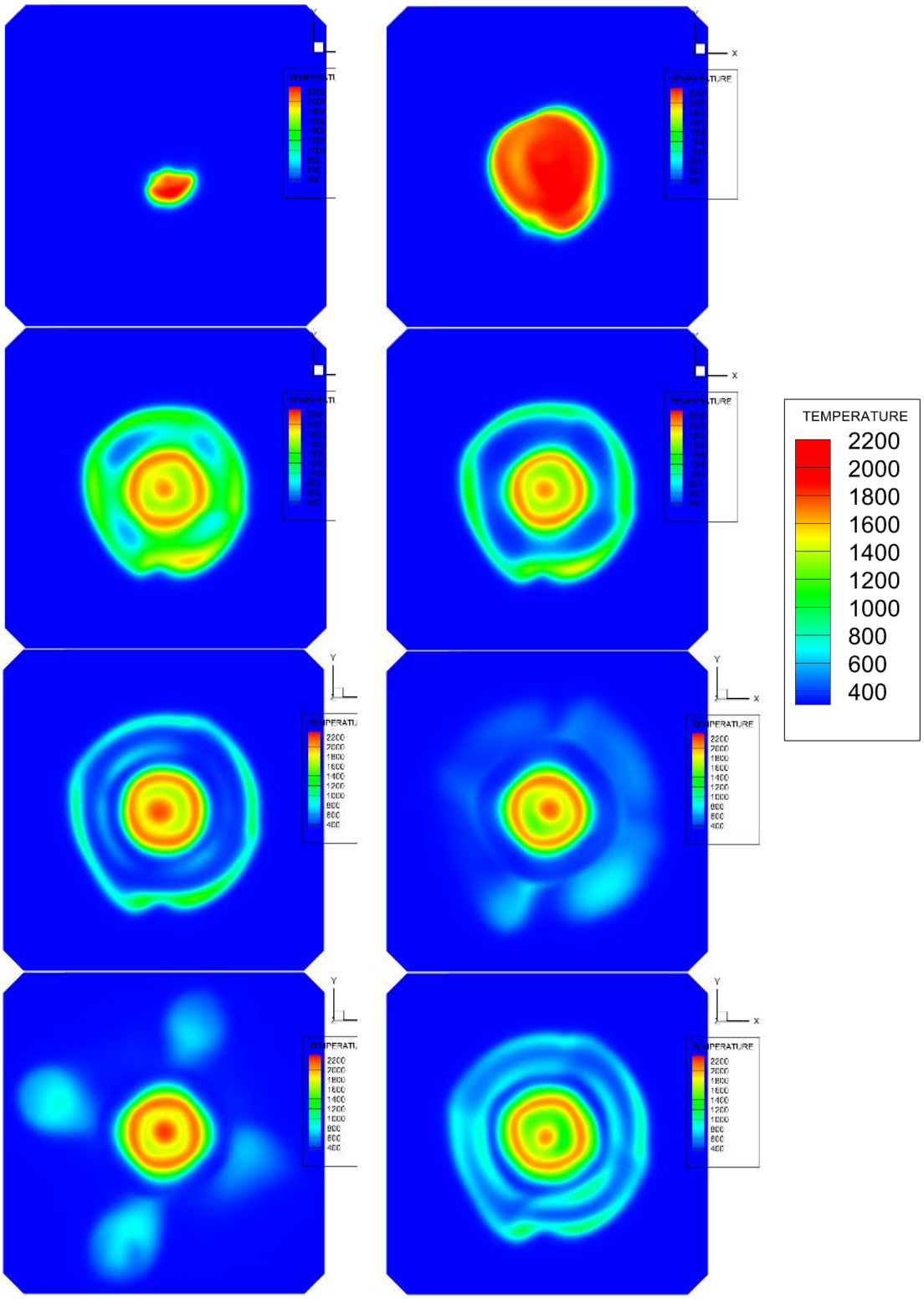

Fig. 11. Instantaneous temperature Contours for attached flame in X-Y plane at Z=15mm from 1-8 ms time step

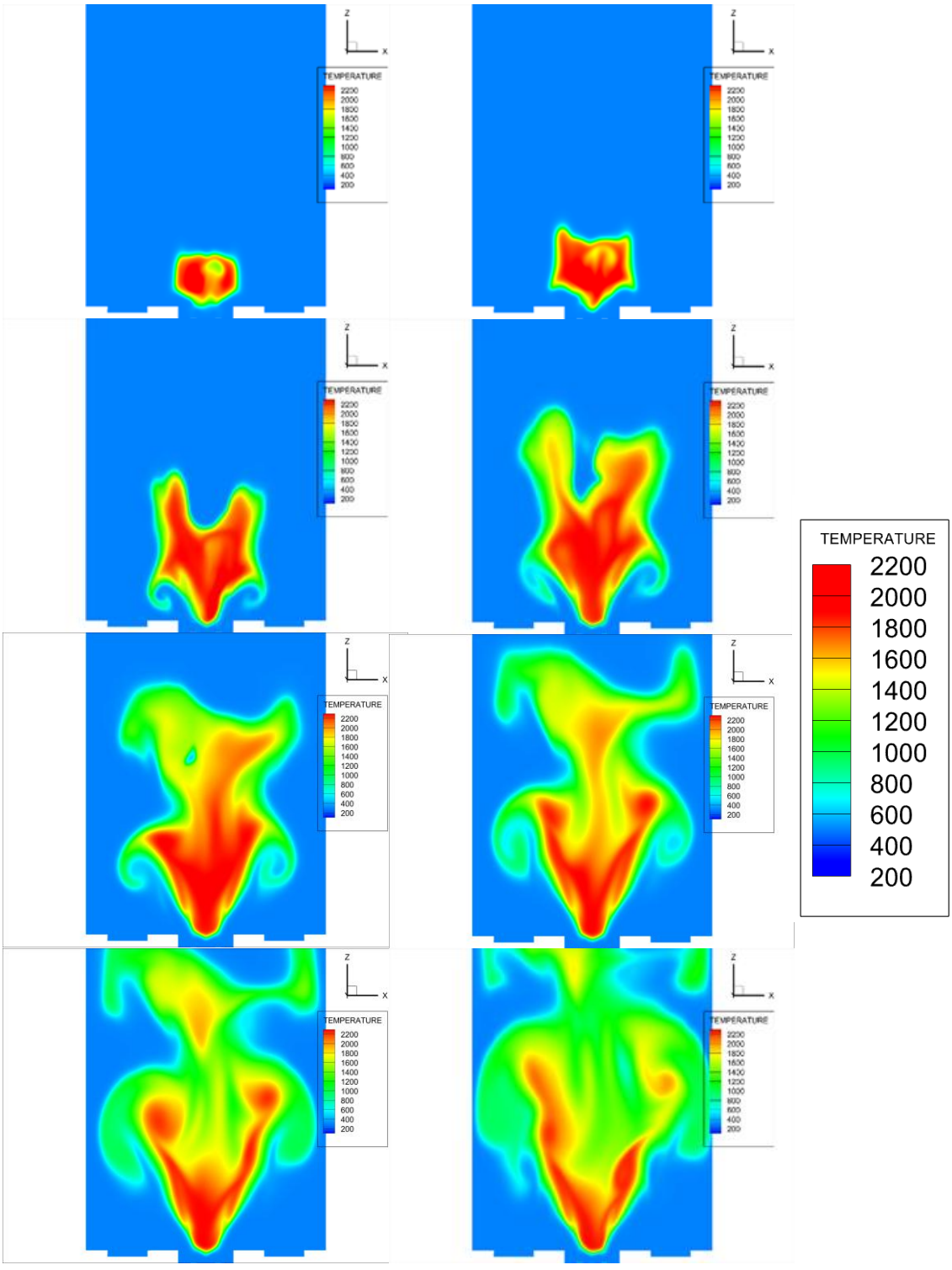

Fig. 12. Instantaneous temperature Contours for lifted flame in Z-X plan at Y=0 from 1-8 ms time step

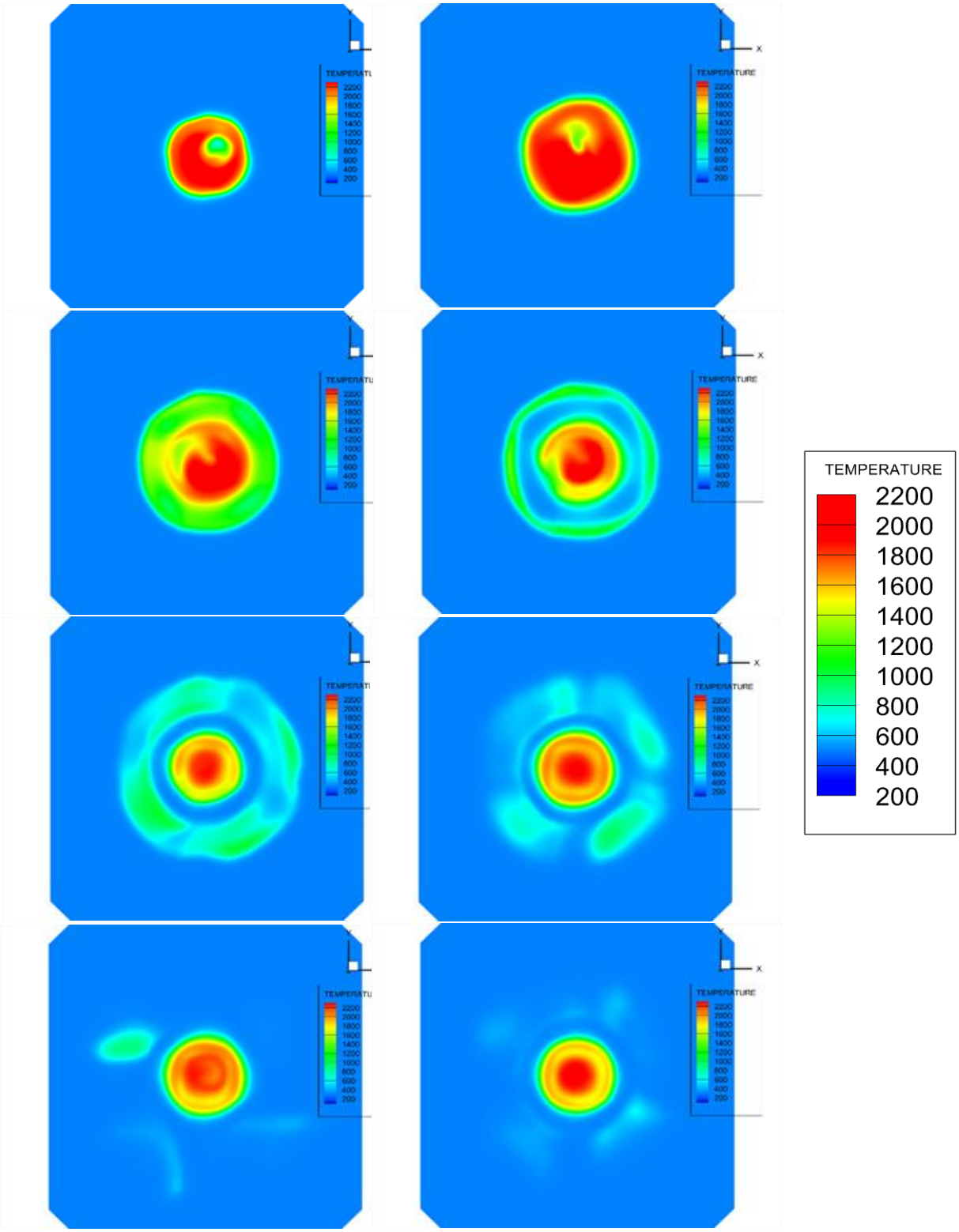

Fig. 13. Instantaneous temperature Contours for lifted flame in X-Y plan at Z=15mm from 1-8 ms time step.

This behavior is more clearly observed in OH distribution as shown in Figure 14, which highlights the flame structure and regions of high reactivity. The OH radical is formed through hydrogen and oxygen reactions in the early stages of combustion. The process begins with the dissociation of hydrogen molecules at high temperatures, leading to the formation of free radicals like H and O, which then react to form OH. This radical serves as a vital indicator of active reaction areas, appearing in regions where chemical reactions are at their most intense. These radicals are generated at high temperatures and in areas with elevated concentrations of fuel and oxygen, making them a crucial tool for understanding flame dynamics and combustion efficiency. OH, concentrations are closely linked to flame stability and efficiency, with high concentrations indicating stable and sustained reactions, while low concentrations may reveal weak reaction areas or potential flame extinction, making OH a key parameter for optimizing combustion system performance.

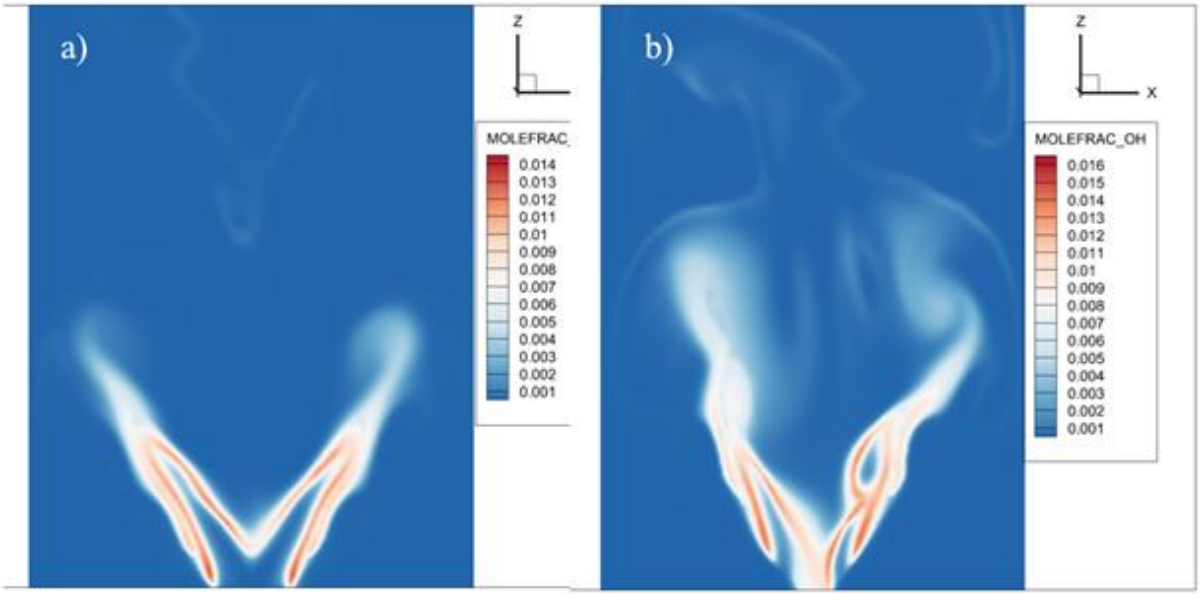

Fig. 14. 2D contour plot of the OH mass fraction for both flames (a) Flame A and (b) Flame L where the flame shape is clearly visible.

NOx Emissions

Figure 15 illustrates the NOx emissions for both flame configurations. The left contour corresponds to the lifted flame (Flame L): while the right contour represents the attached flame (Flame A). In the lifted flame (Flame L): NOx emissions are significantly lower and more distributed due to the flame's V shape, which enhances fuel-air mixing before combustion and reduces residence time at high temperatures. This combination suppresses NOx formation by limiting the conditions conducive to the thermal Zeldovich mechanism. Additionally, observations suggest that NOx formation is not concentrated at the primary reaction front but rather in secondary regions within high-temperature zones. This aligns with studies showing that NOx emissions are influenced by both residence time and peak flame temperature (Hwang et al., 2007; Wang & Yang, 2024). The lifted flame's gap between the flame base and the injector mitigates these factors by promoting a more even thermal distribution, which reduces localized hot zones and their associated NOx formation via the thermal Zeldovich mechanism.

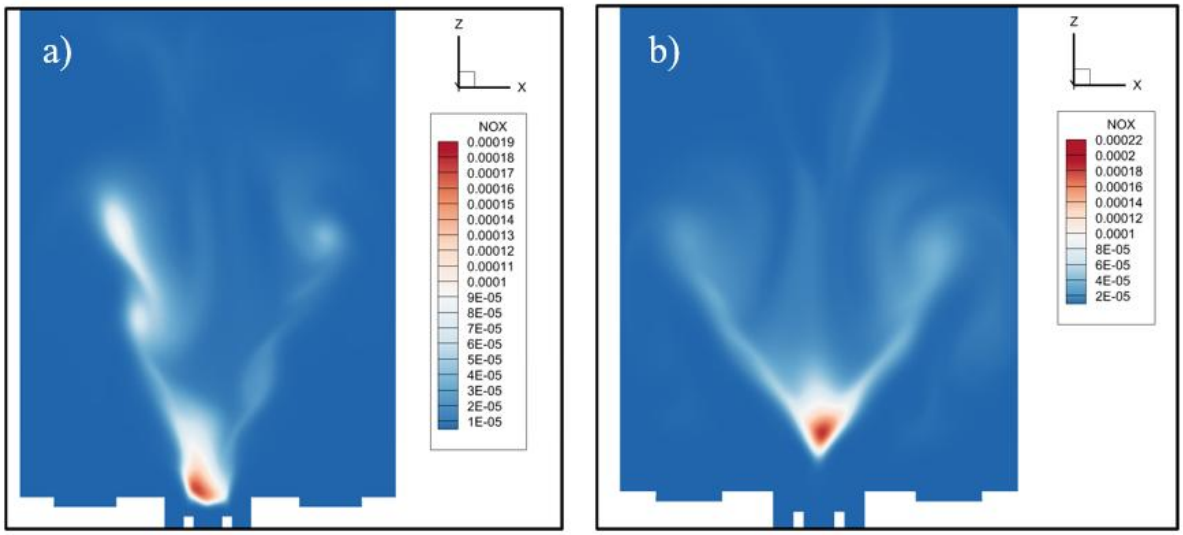

Fig. 15. Comparison of the NOx concentration in a) flame L and b) flame A.

In contrast, the attached flame (Flame A) shows higher NOx emissions concentrated away the injector nozzle. This phenomenon arises from the extended residence time of hot gases within the central recirculation zone (CRZ): where intense thermal reactions are sustained. The CRZ serves as a containment area for hot combustion products, allowing them to remain in high-temperature zones for longer periods, thereby facilitating NOx formation through the thermal Zeldovich mechanism. Additionally, NO production is observed predominantly in secondary high-temperature regions, rather than directly at the primary reaction front, a behavior linked to the recirculation dynamics. The M shape of the flame further amplifies these effects by creating localized hotspots near the stabilization region, where thermal gradients and prolonged residence times converge to accelerate NOx generation. These findings highlight the significant influence of the CRZ on emissions and emphasize the necessity of controlling residence time and thermal gradients to mitigate NOx production effectively.

Turbulence Flame Interaction

In Large Eddy Simulation (LES): subgrid-scale turbulent viscosity is a crucial modeling concept used to account for the effects of small, unresolved turbulent eddies that are filtered out in the simulation. This viscosity dissipates energy at smaller scales, ensuring numerical stability and accurately representing turbulent dynamics. Figures 16 and 17 demonstrate the development of turbulent viscosity at a specific combustion phase, where it serves as an indicator of turbulent intensity. Regions with high flow velocities develop higher turbulent viscosity due to the pronounced velocity gradients in these areas, as velocity vanishes near the chamber walls. The most significant turbulent viscosity is observed inside the nozzle of the combustion chamber, where the swirl flow intensifies. This is a result of rapid velocity variations caused by swirling motion, which amplifies energy dissipation. Similarly, subgrid-scale turbulent kinetic energy (SGS TKE) quantifies the kinetic energy of small, unresolved eddies. It plays a vital role in turbulence models, to capture energy transfer between resolved and unresolved scales. Proper modeling of SGS TKE enhances the representation of the energy

cascade and turbulence dynamics, ensuring accurate energy dissipation and distribution. The patterns of SGS TKE closely align with turbulent viscosity, as regions of higher viscosity typically correspond to increased SGS TKE. The results also conclude that high swirl intensity develops near the chamber exit due to thermal expansion effects. The flow accelerates as the mixture's density decreases in high-temperature regions downstream, further intensifying turbulence. These insights highlight the importance of both turbulent viscosity and SGS TKE in accurately capturing complex flow and combustion processes.

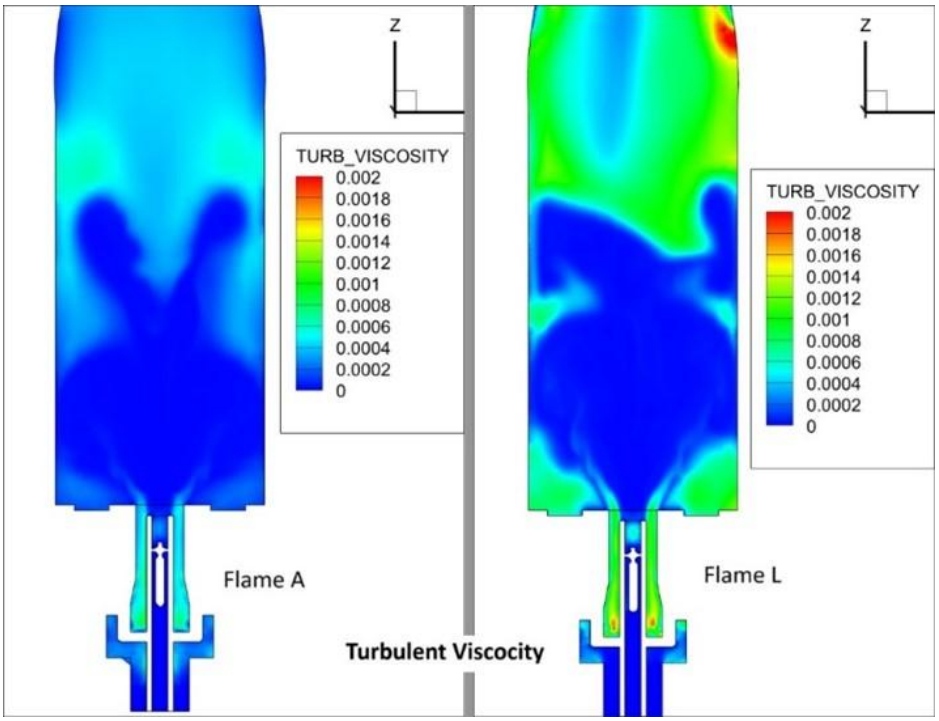

Fig. 16. Developed turbulent viscosity for (A) Flame A, and (B) Flame L.

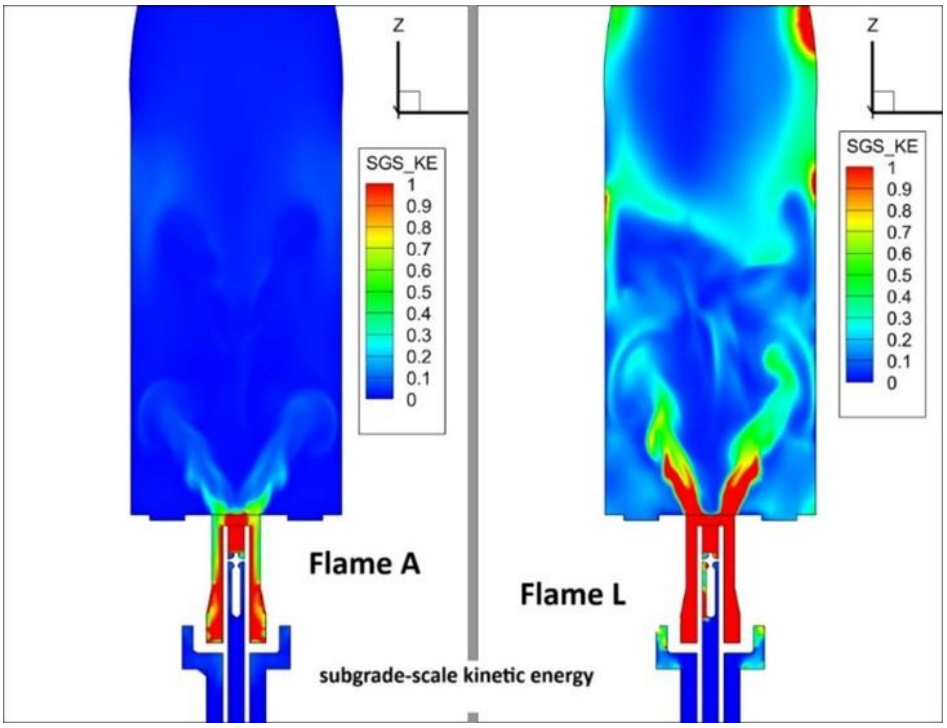

Fig. 17. Developed subgrade-scale kinetic energy for (A) Flame A, and (B) Flame L.

CONCLUSION

Studies on non-premixed swirl-stabilized hydrogen flames using Large Eddy Simulation (LES) are of significant importance due to the complex technical challenges associated with flame stabilization, combustion efficiency, and NOx emission control. This work aims to address these challenges by providing a detailed analysis of non-premixed hydrogen flames under swirl-stabilized conditions, focusing on the role of recirculation zones (CRZ and ORZ) in determining flame structure, stability, and pollutant formation, utilizing LES as the primary computational tool. A three-dimensional LES model was developed to simulate turbulent hydrogen combustion and was validated against experimental data obtained through Particle Image Velocimetry (PIV). The study investigated two distinct flame types: the attached flame, which anchors directly at the injector exit, and the lifted flame, which stabilizes downstream at a certain distance from the injector. Particular attention was given to evaluating the flame stabilization mechanisms, fuel-air mixing quality, and thermal NOx formation via the Zeldovich mechanism.

The main conclusions drawn from the study are as follows:

1. Central (CRZ) and outer recirculation zones (ORZ) play a fundamental role in shaping flame morphology, enhancing stabilization, and influencing pollutant emission behavior.
2. The lifted flame shows better performance in terms of stability and lower NOx emissions because it allows for better mixing between fuel and air. On the other hand, the attached flame produces higher NOx emissions due to the longer residence time of gases in high-temperature regions, which leads to more NOx formation through the thermal Zeldovich mechanism.
3. Optimization of fuel injection techniques and operating conditions is essential for achieving stable and low-emission hydrogen combustion in practical systems.

4. The LES model proved highly accurate in predicting flow fields, flame structures, and pollutant formation mechanisms, validating its effectiveness as a diagnostic and predictive tool for turbulent hydrogen combustion analysis.
5. Further enhancement of LES frameworks through the integration of detailed chemical kinetic mechanisms is recommended to improve the prediction of hydrogen oxidation pathways and NOx formation dynamics, thereby supporting the development of next-generation clean and sustainable combustion technologies.

REFERENCES

Aniello, A., Laera, D., Marragou, S., Magnes, H., Selle, L., Schuller, T., & Poinsot, T. (2023). Experimental and numerical investigation of two flame stabilization regimes observed in a dual swirl H_2-air coaxial injector. Combustion and Flame, 249, 112595.

Beér, J. M., & Chigier, N. A. (1972). Combustion aerodynamics. Fuel and Energy Science Series. Applied Science Publishers.

Bouvet, N., Halter, F., Chauveau, C., & Yoon, Y. (2013). On the effective Lewis number formulations for lean hydrogen/hydrocarbon/air mixtures. International Journal of Hydrogen Energy, 38(14), 5949–5960.

Capurso, T., Laera, D., Riber, E., & Cuenot, B. (2023). NOx pathways in lean partially premixed swirling H_2-air turbulent flame. Combustion and Flame, 248, 112581.

Chiesa, P., Lozza, G., & Mazzocchi, L. (2005). Using hydrogen as gas turbine fuel. Journal of Engineering for Gas Turbines and Power, 127(1), 73–80.

Chigier, N. A., & Beer, J. M. (1964). Velocity and static-pressure distributions in swirling air jets issuing from annular and divergent nozzles.

Chigier, N. A., & Chervinsky, A. (1967). Aerodynamic study of turbulent burning free jets with swirl. In Symposium (International) on Combustion (Vol. 11, No. 1, pp. 489–499). Elsevier.

Chigier, N. A., & Chervinsky, A. (1967). Experimental investigation of swirling vortex motion in jets.

Dincer, I. (2012). Green methods for hydrogen production. International Journal of Hydrogen Energy, 37(2), 1954–1971.

Duan, Z., Shaffer, B., McDonell, V., Baumgartner, G., & Sattelmayer, T. (2014). Influence of burner material, tip temperature, and geometrical flame configuration on flashback propensity of H_2-air jet flames. Journal of Engineering for Gas Turbines and Power, 136(2), 021502.

Ebi, D., Bombach, R., & Jansohn, P. (2021). Swirl flame boundary layer flashback at elevated pressure: Modes of propagation and effect of hydrogen addition. Proceedings of the Combustion Institute, 38(4), 6345–6353.

Eichler, C., & Sattelmayer, T. (2012). Premixed flame flashback in wall boundary layers studied by long-distance micro-PIV. Experiments in Fluids, 52(2), 347–360.

Fairweather, M., Ormsby, M. P., Sheppard, C. G. W., & Woolley, R. (2009). Turbulent burning rates of methane and methane–hydrogen mixtures. Combustion and Flame, 156(4), 780–790.

Galley, D., Ducruix, S., Lacas, F., & Veynante, D. (2011). Mixing and stabilization study of a partially premixed swirling flame using laser induced fluorescence. Combustion and Flame, 158(1), 155–171.

Gupta, A. (2000). Flame characteristics with high temperature air combustion. In 38th Aerospace Sciences Meeting and Exhibit (p. 593).

Gupta, A. K., Bolz, S., & Hasegawa, T. (1999). Effect of air preheat temperature and oxygen concentration on flame structure and emission.

Gupta, A. K., Lilley, D. G., & Syred, N. (1984). Swirl flows. Tunbridge Wells.

Hwang, C. H., Hyun, S. H., Tak, Y. J., & Lee, C. E. (2007). The effect of residence time and heat loss on NOx formation characteristics in the downstream region of CH_4/air premixed flame. Transactions of the Korean Society of Mechanical Engineers B, 31(1), 99–108.

IEA. (2022). World energy outlook 2022. International Energy Agency.

İlbaş, M., Karyeyen, S., & Yilmaz, İ. (2016). Effect of swirl number on combustion characteristics of hydrogen-containing fuels in a combustor. International Journal of Hydrogen Energy, 41(17), 7185–7191.

Jensen, L. (2020). EU climate target plan: Raising the level of ambition for 2030.

Kim, M., Waddell, K. A., Sunderland, P. B., Nayagam, V., Stocker, D. P., Dietrich, D. L., ... & Axelbaum, R. L. (2023). Spherical gas-fueled cool diffusion flames. Proceedings of the Combustion Institute, 39(2), 1647–1656.

Lan, Y., Wang, Z., Xu, J., & Yi, W. (2024). The impact of hydrogen on flame characteristics and pollutant emissions in natural gas industrial combustion systems. Energies, 17(19).

Lipatnikov, A. N., & Sabelnikov, V. A. (2020). An extended flamelet-based presumed probability density function for predicting mean concentrations of various species in premixed turbulent flames. International Journal of Hydrogen Energy, 45(55), 31162–31178.

Lu, C., Zhang, L., Chen, X., Xing, C., Liu, L., Shi, H., & Qiu, P. (2023). The effects of steam dilution on flame structure and stability for a H_2/air micromix burner. Journal of the Energy Institute, 107, 101188.

Marragou, S. (2023). Flow structure, mixing, flame stabilization and pollutant emissions from a coaxial dual swirl CH_4/H_2/air injector [Doctoral dissertation, Institut National Polytechnique de Toulouse-INPT].

Martinez, D. M., & Jiang, X. (2013). Large-eddy simulations of unsteady hydrogen annular flames. Computers & Fluids, 80, 429–440.

Menon, S., Yeung, P. K., & Kim, W. W. (1996). Effect of subgrid models on the computed interscale energy transfer in isotropic turbulence. Computers & Fluids, 25(2), 165–180.

Milton, B. E., & Keck, J. C. (1984). Laminar burning velocities in stoichiometric hydrogen and hydrogen/hydrocarbon gas mixtures. Combustion and Flame, 58(1), 13–22.

Otway, N. (2020). Large Eddy Simulation Techniques for Predicting Turbulent Combustion of Hydrogen Fuel.

Patel, V., & Shah, R. (2019). Effect of hydrogen enrichment on combustion characteristics of methane swirling and non-swirling inverse diffusion flame. International Journal of Hydrogen Energy, 44(52), 28316–28329.

Reichel, T. G., & Paschereit, C. O. (2017). Interaction mechanisms of fuel momentum with flashback limits in lean-premixed combustion of hydrogen. International Journal of Hydrogen Energy, 42(7), 4518–4529.

Reichel, T. G., Terhaar, S., & Paschereit, O. (2015). Increasing flashback resistance in lean premixed swirl-stabilized hydrogen combustion by axial air injection. Journal of Engineering for Gas Turbines and Power, 137(7), 071503.

Richards, K. J., Senecal, P. K., & Pomraning, E. (2023). Converge 3.2. Convergent Science.

Shahin, Z. (2024). Large-Eddy Simulation of Turbulent Swirling Flame in a Dual Swirl H_2-Air Coaxial Injector.

Sommerer, Y., Galley, D., Poinsot, T., Ducruix, S., Lacas, F., & Veynante, D. (2004). Large eddy simulation and experimental study of flashback and blow-off in a lean partially premixed swirled burner. Journal of Turbulence, 5(1), 037.

Truffin, K., Luca, P. G., Ho, T. N. D., Bertsch, J., Maio, G., Mehl, C., ... & Taddeo, L. (2024, April). Large-eddy simulation and experimental study of a partially premixed hydrogen/air swirled burner: Impact of the injection system. In INFUB-14.

Tummers, M. J., Hübner, A. W., Van Veen, E. H., Hanjalić, K., & Van der Meer, T. H. (2009). Hysteresis and transition in swirling nonpremixed flames. Combustion and Flame, 156(2), 447–459.Wang, Z., & Yang, X. (2024). NOx Formation Mechanism and Emission Prediction in Turbulent Combustion: A Review. Applied Sciences (2076-3417), 14(14).

Yoshizawa, A., & Horiuti, K. (1985). A statistically-derived subgrid-scale kinetic energy model for the large-eddy simulation of turbulent flows. Journal of the Physical Society of Japan, 54(8), 2834–2839.

Zhen, H. S., Leung, C. W., & Cheung, C. S. (2010). Thermal and emission characteristics of a turbulent swirling inverse diffusion flame. International Journal of Heat and Mass Transfer, 53(5–6), 902–909.